AIAA SciTech Forum
11–15 & 19–21 January 2021, VIRTUAL EVENT
AIAA Scitech 2021 Forum

10.2514/6.2021-1560

Study of Axial Groove Casing Treatment for Co-Flow Jet Micro-Compressor Actuators

Kewei Xu *, Gecheng Zha †
Dept. of Mechanical and Aerospace Engineering
University of Miami, Coral Gables, Florida 33124
E-mail: gzha@miami.edu

Abstract

This paper conducts numerical trade study of the axial groove (AG) casing treatment for micro-compressor actuators used for Co-Flow Jet (CFJ) active flow control. The purpose is to increase the stall margin for the micro-compressors while minimizing the design point efficiency penalty. Three geometrical parameters are varied for the trade study, including: width, length and skew angle. The numerical approach is validated with a tested micro-compressor using recirculating casing treatment. A very good agreement is achieved between the predicted speedlines and the measured results for the validated micro-compressor. For the width study, wide width with W/P of 60% possesses a higher stall margin improvement (SMI) of 10.1%, but an increased design point efficiency penalty of 4% also occurs. To preserve micro-compressor efficiency, the width W/P of 30% is adopted that has SMI of 3.1% with efficiency reduced by only 1.1%. Decreasing AG length to 0.7C (chord) results in a reduction of efficiency penalty while maintaining a similar SMI. However, a further decrease of AG length to 0.6C significantly hurts stall margin and reduces SMI by half. For the skew angle study, 52.5° is the optimal angle for AG to extract tip flow, which substantially enhances flow re-circulation and mitigates tip blockage. Overall, the optimum AG has the upstream point located at 0.2C ahead of LE and downstream point at 0.5C after the LE and has a W/P of 30%, a length of 0.7C with a skew angle of 52.5°. The micro-compressor with the optimum AG configuration is able to improve stall margin by 7.4% with a design point efficiency penalty of 0.6%.

Nomenclature

CFJ	Co-Flow jet
AG	Axial Groove
AoA	Angle of Attack
D	Diameter
TE	Trailing Edge
LE	Leading Edge
L	Length
OGV	Outlet Guide Vane
P	Pitch
$RANS$	Reynolds-Averaged Navier-Stokes
RPM	Round per Minute
R_e	Reynolds Number

* Ph.D. Candidate
† Professor, AIAA associate Fellow

RCT	Recirculating Casing Treatment
$ZNMF$	Zero-Net Mass Flux
AFC	Active Flow Control
$\dot{m}$	Mass Flow
m_{cor}	Corrected Mass Flow Rate
Ma	Mach Number
U	Circumferential Speed
W	Width
SMI	Stall Margin Improvement
c	Subscript, stands for corrected
j	Subscript, stands for jet
0	Total
1	Impeller Inlet
2	Impeller Outlet
t	Tip
$s-t$	Static to Total
α	Skew Angle
ω	Rotational Speed
γ	Air specific heats ratio
τ	Shear Stress
η	CFJ pumping system efficiency, propeller efficiency
π	Pressure Ratio
θ	Extraction angle

1 Introduction

Co-Flow Jet is a zero-net mass-flux (ZNMF) active flow control (AFC) method recently developed by Zha et al.[1, 2, 3, 4, 5, 6, 7, 8] that has micro-compressors embedded inside the airfoil as actuators (Fig. 1). A CFJ airfoil withdraws flow from trailing edge, pressurizes it by the micro-compressor, and re-injects flow at leading edge. It is demonstrated numerically and experimentally that CFJ achieves radical lift augmentation, drag reduction and stall angle of attack increase. The mixed type compressor is preferred to be used as the CFJ actuator due to its compact size and high flow capacity [8, 9, 10, 11, 12].

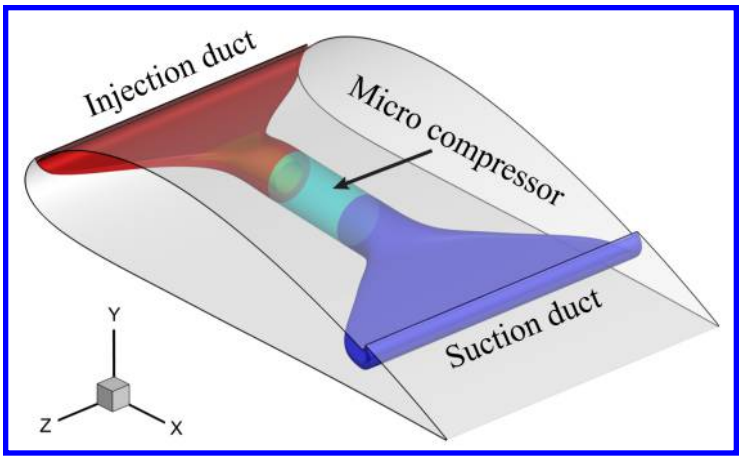

Figure 1: Schematics of the CFJ airfoil with embedded micro-compressor

In order to be operated in a wide flight envelope, the micro-compressor is required to have large operating range. Axial groove (AG) casing treatment [13, 14, 15] is proved to be advantageous to extend the micro-compressor stall margin with simple structure. The AG connects the blade tip separation zone with the upstream main flow, which mitigates the tip blockage. It is able to achieve a significant stall margin improvement (SMI) with a small efficiency loss at the design point, and is therefore being studied widely.

Fujita et al [16] test a series of configurations of casing treatment to investigate the relation between the stall margin improvement (SMI) and the compressor efficiency. The results show that it is inevitable to have efficiency loss for stall margin improvement using casing treatment. Wilke et al [17] numerically study the effects of the axial slots position using time-accurate simulations. The axial slots extending more upstream demonstrates a higher efficiency than the slots locating more downstream. The fundamental mechanisms of casing treatment are studied by Lu et al [18]. They found that the end-wall casing treatment significantly mitigates or removes the blockage near the upstream part of the blade passage and improves rotor stall margin. A systematic numerical study is conducted by Noureddine et al [19] to investigate the casing treatment slot geometry effects on the performance of a mixed-flow rotor. The results indicate that the geometrical parameters having a large impact on the compressor performance include: open area ratio, slot skew angle, slot axial length and slot axial position. Juan et al [20] study the axial groove and circumferential groove on a mixed flow compressor. The circumferential groove does not have a notable effect on compressor performance compared with the axial groove, which substantially extends flow range but comes with a higher efficiency loss. The optimum axial groove with the open area ratio of 20% achieves 14% of SMI and 1% of efficiency penalty. Axial groove casing treatment is also applied to a centrifugal compressor shroud by Harley et al [21]. The results suggest that axial grooves at the impeller inlet are an effective method of improving the surge margin with a small penalty on efficiency.

In our previous studies [8, 9, 10, 12, 22], the recirculating casing treatment (RCT) is implemented on the micro-compressors with designed total pressure ratio of 1.2 [9, 10, 12] and 1.095 [22], which achieves significant SMI with limited efficiency penalty. The axial groove casing treatment configuration is easier for manufacturing than the RCT, which is attractive if a similar performance enhancement can be achieved. The propose of this paper is to apply the axial groove casing treatment on the micro-compressor to investigate its effectiveness for improving compressor performance. The studied geometrical parameters for axial groove include width, length and skew angle (α).

2 Computational Setup

The geometry of the micro-compressor with axial groove (AG) applied is shown in Fig. 2, where pitch (P), width (W), length (L), and skew angle (α) are marked for the AG. The skew angle (α) measures the angle of the AG to the radial direction. The AG length is always along the axial direction.

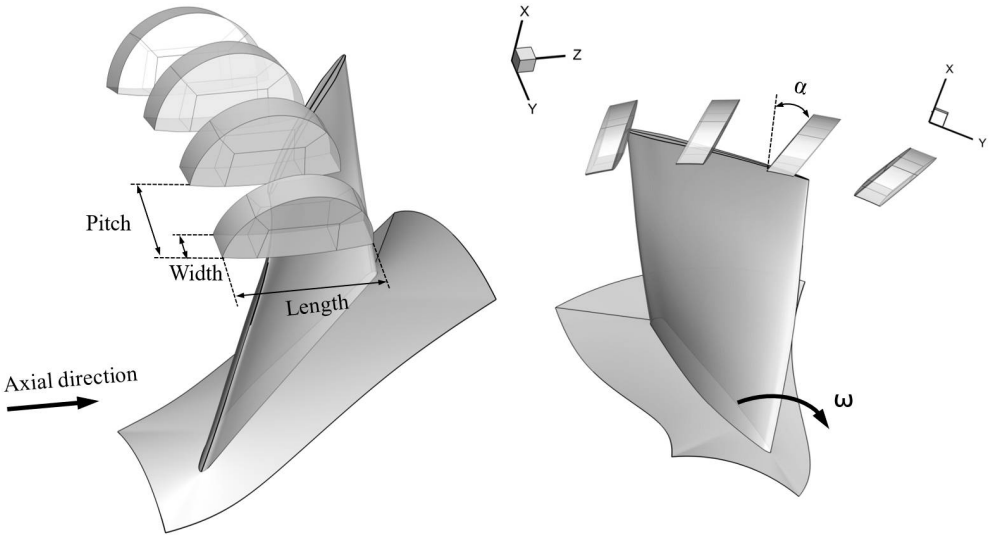

Figure 2: Illustration of the micro-compressor axial groove

As shown in Fig. 3, the computational domain has a single blade passage, which consists of a converging intake, an impeller passage and an axial groove casing treatment. The intake and impeller passage are meshed using structured grid in Turbogrid with a size of 0.58 million points. The impeller blade is meshed using O-grid topology, which has 42 points in the blade span, 12 points at tip gap and 199 points around the blade. The wall spacing is set to make y^+ close to 1. The axial groove casing treatment is meshed using structured grid with butterfly topology for the semi-circle wall. The mesh has 0.54 million points, and the mesh refinement study indicates that the results are converged based on the mesh size.

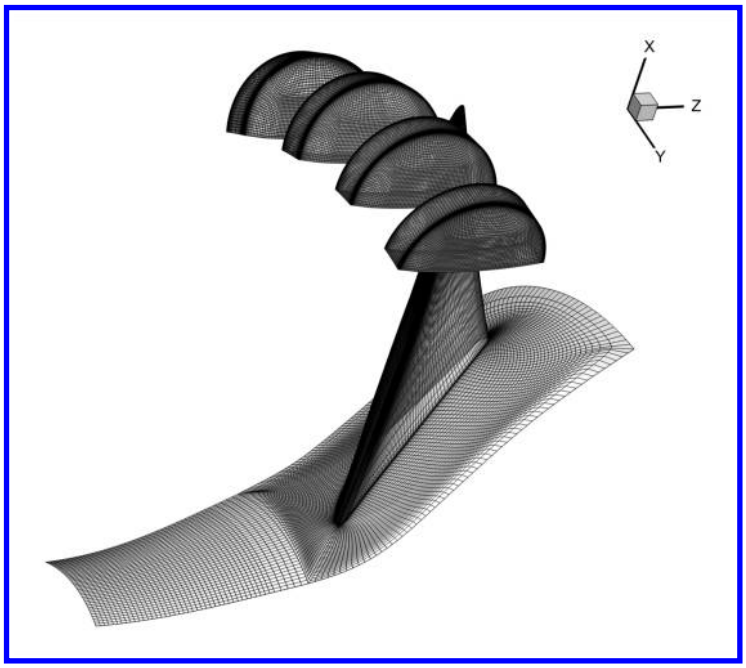

Figure 3: Computational domain of the micro-compressor simulation

The 3D Reynolds Averaged Navier-Stokes (RANS) equations are solved using ANSYS CFX code. The k-ω shear stress transport (SST) turbulent model is adopted. The advection terms are solved with 2nd order scheme. Total pressure, total temperature and flow direction are specified as inlet boundary conditions. Target exit mass flow rate is used as the outlet boundary condition to obtain the stable solutions at near stall. Non-slip wall boundary condition is imposed on all solid walls. The frozen rotor boundary condition is applied on the interface between casing treatment and compressor casing. The interface between intake and impeller is treated with stage mixing boundary condition. The convergence criterion is that the residual reduced by 4 orders of magnitude. In the near stall condition, such criterion is difficult to reach due to the instability of the stalled flow in the casing treatment. Therefore, the computation is considered as converged when the mass flow becomes dynamically stable with time.

3 Validation of the Micro-Compressor with Casing Treatment

A rig tested, mixed-flow micro-compressor with recirculating casing treatment (RCT) utilized in our previous CFJ airfoil studies [8, 9, 10, 12] is used to validate the numerical approach, shown in Fig. 4. RCT improves stall margin using the similar mechanism with axial groove, extracting vortical flow from blade tip passage downstream and re-injecting in the upstream, and is therefore used here for validation. Fig. 5 shows the streamlines in the RCT slot and ducts of the validated micro-compressor at near stall. The validated compressor has the similar size and Reynolds number of 92000 with the micro-compressor studied in this paper. However, it has lower mass flow rate and a higher total pressure ratio (P_{tr}). Its design point has total pressure ratio of 1.21 and isentropic efficiency of 80.2%. The computed speedlines with the pressure ratio and efficiency are in good agreement with the measurements [10] as shown in Fig. 6, which has the mass flow rate normalized by the design point mass flow rate.

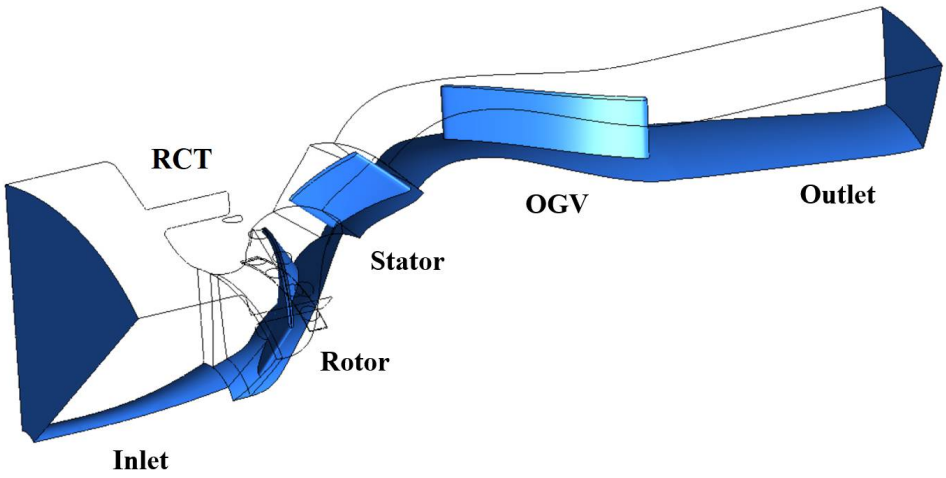

Figure 4: The configuration of the validated micro-compressor

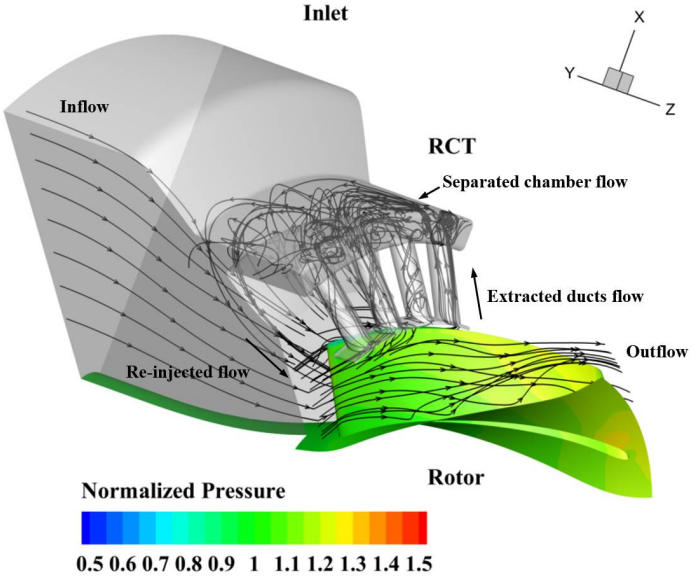

Figure 5: Streamlines and static pressure contour of the validated micro-compressor at near stall

The maximum discrepancy between the computed and measured pressure ratio and isentropic efficiency at near stall are 2.32% and 2.1% respectively. The discrepancy is mostly due to the flow separation and complex vortical flow at near stall condition, for which the RANS turbulence model is inadequate to resolve. Overall, the computed results agrees well with experimental data and the present computational setup is adopted for the axial groove casing treatment simulation.

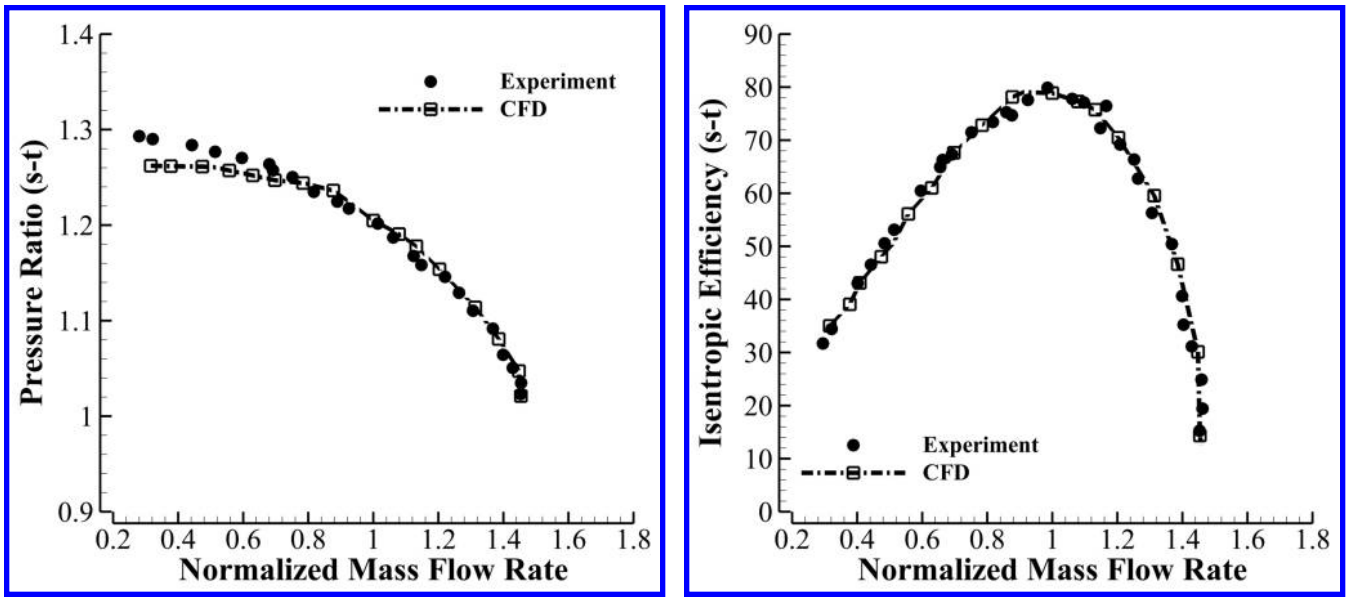

(a) Pressure ratio (b) Isentropic efficiency

Figure 6: Computed speedlines of a micro-compressor compared with the measured results [10]

4 The Baseline Micro-compressor

The baseline mixed-type single rotor micro-compressor with no casing treatment is designed following the procedure described in [11]. The front loading work distribution is adopted for the impeller blade at low span to reduce boundary layer loss. Double circular arc (DCA) blade shape with rear loading work distribution is used for the design of the tip blade to mitigate shock wave. Hub strong work distribution is applied for the rotor span to reduce hub loading for downstream diffuser. The rotor designed efficiency achieves 90.6% with a total pressure ratio of 1.185 and a high mass flow rate. The main geometrical parameters of the baseline micro-compressor is presented in the Table 1.

Table 1: Rotor Geometrical Parameters

Rotor inlet hub diameter	16.0mm
Rotor inlet casing diameter	43.3mm
Number of impeller blades	8

Fig. 7 presents the computed speedlines at two normalized RPM ($n/\sqrt{T_{01}}$), 7420 and 7990. The designed speedline is at 7420, which provides the required mass flow rate and pressure ratio for co-flow jet airfoil flow control at cruise condition. The designed speedline of the baseline micro-compressor has 27.8% of stall margin defined by Eq. (1) and the AG geometry studies are conducted for the designed RPM.

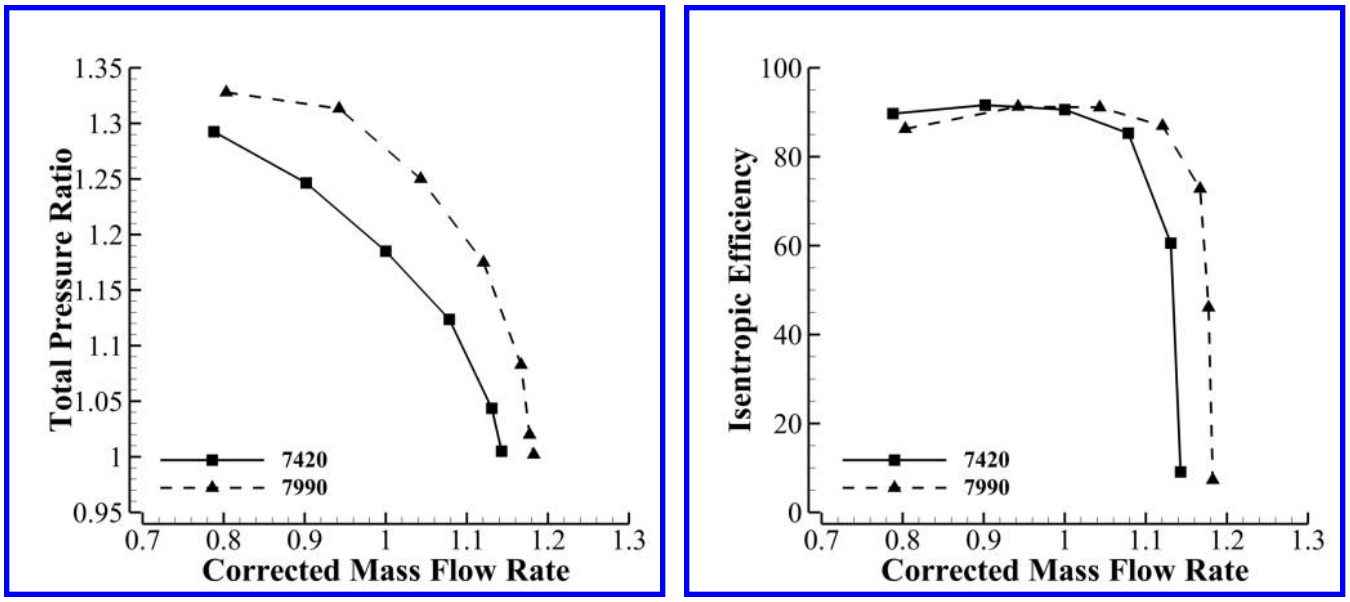

(a) Total pressure ratio (b) Isentropic efficiency

Figure 7: Computed speedlines of the baseline micro-compressor

The stall margin is defined as:

$$SM = 1 - \left[\frac{(p_{02}/p_{01})_{design}}{(p_{02}/p_{01})_{stall}} \times \frac{m_{cor-stall}}{m_{cor-design}} \right] \tag{1}$$

where m_{cor} is the corrected mass flow rate defined by $\dot{m}\dfrac{\sqrt{T_0}}{p_0}$.

5 Results of Axial Groove Casing Treatment

This section presents the results of the micro-compressor with various axial groove configurations. The casing treatment is designed with four axial grooves for each blade passage. The number of grooves and locations are selected based on the previous experience [22]. Three geometrical parameters of the AG are studied, namely: width (W), length (L) and skew angle (α). The goal is to obtain the optimum configuration of the axial groove casing treatment that achieves significant stall margin improvement with a minimum design point efficiency penalty. The initial AG is semi-circle shape that has a length of 1 chord of the blade tip axial chord, a skew angle α of 0° and a width of W/P=60%, where W/P is the ratio of width to pitch.

5.1 Width Study

Two AG width are studied, W/P of 60% and 30%, and are labeled Case 1 and Case 2. Both configurations has the same AG axial location, which starts at half chord ahead of the LE of tip blade and ends at the mid-chord of the tip blade. Fig. 8 shows the performance comparison between the baseline micro-compressor and the micro-compressors with the two AG applied with length of 1C. Significant stall margin improvement of about 10.1% is

achieved for the Case 1 with W/P of 60%, whereas the Case 2 with W/P of 30% only increases the stall margin by about 3.1%. This is because a wider groove allows more mass flow to be extracted from the separated region at tip and be transferred to the upstream, which is more effective to reduce tip blockage. However, this advantage of the stall margin increase is a disadvantage to hurt the design point efficiency, because a wider groove also passes more mass flow at design point. Case 1 has its isentropic efficiency reduced by 4%, whereas Case 2 only has a penalty of 1.1%. The micro-compressor is designed to mostly work in a cruise condition and preserving efficiency is very important. Therefore, Case 2 with the W/P of 30% is accepted as the more desirable design.

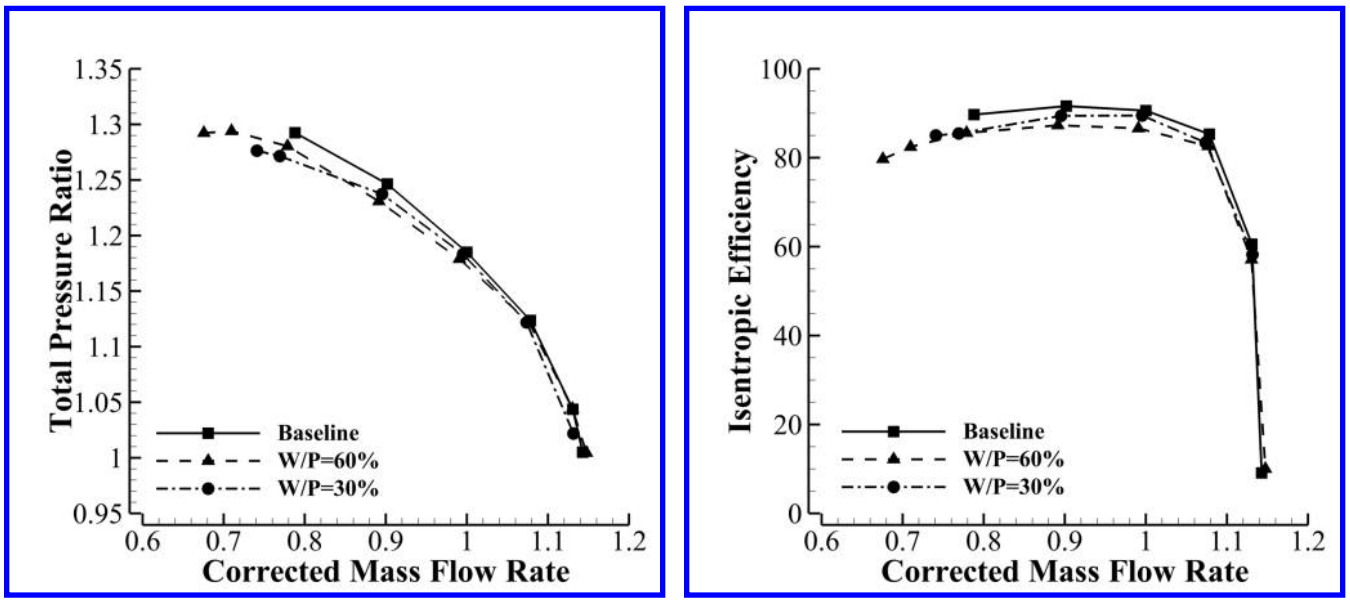

(a) Total pressure ratio (b) Isentropic efficiency

Figure 8: Computed speedlines of the axial groove with various width

5.2 Length Study

This section study the length effect of axial groove on stall margin improvement. Two length of AG are studied, 0.6C and 0.7C and labeled as Case 3 and 4. Both cases has the groove downstream point at the half chord ahead of the tip blade with the W/P of 30% adopted from the previous study. The groove shape is fixed with semi-circle. Fig. 9 compares the compressor characteristic curves of Case 2, 3 and 4 with the baseline micro-compressor. At near stall point, about 3.4% of stall margin improvement is achieved in Case 4, whereas Case 3 only achieves 1.7%. For the design point efficiency penalty, Case 3 has a reduction of 0.6%, which is lower than that of Case 4 of 0.9%. This is because a longer AG length extends more upstream at the low pressure region so that the pressure difference between extraction and re-injection can be achieved, which allows higher mass flow rate to be recirculated to the upstream. At the design point, the enhanced recirculated flow is a waste of compressor work and therefore reduces efficiency. At the near stall, tip blockage is effectively inhibited due to a higher recirculated flow rate, which contribute to larger stall margin.

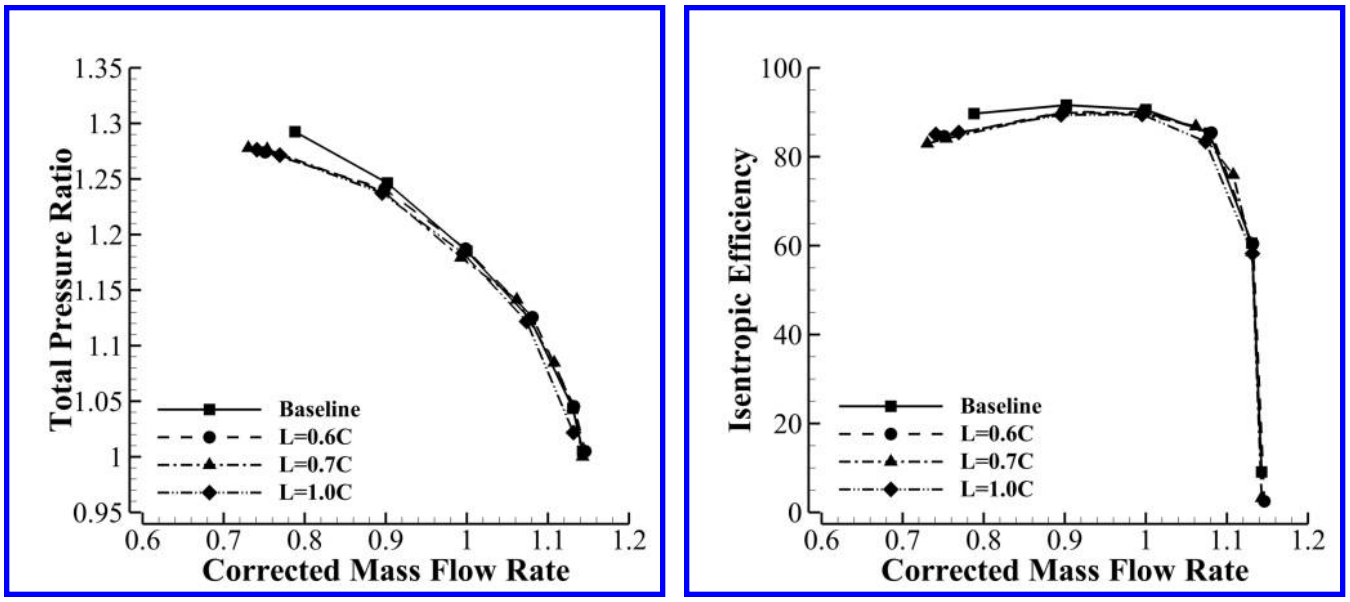

(a) Total pressure ratio (b) Isentropic efficiency

Figure 9: Computed speedlines of the axial groove with various length

Fig. 10 shows the Mach number contours at span 98% of Case 3 and Case 4 at near stall condition. The high Mach number zone near blade leading edge in Case 4 is enlarged compared to Case 3 due to the more reduced flow blockage. The groove length of 0.7C with a higher SMI is adopted as the desirable AG length and is used for the following trade study.

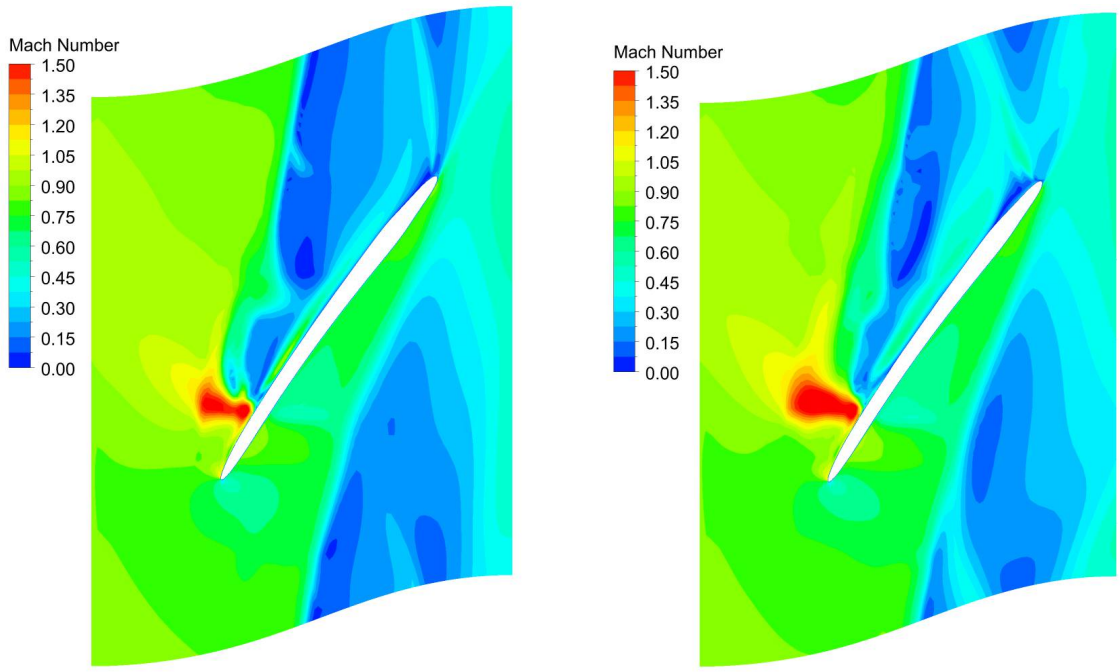

(a) Case 3 (b) Case 4

Figure 10: Mach number distribution at near casing

5.3 Skew Angle Study

Fig. 11 shows three cases with respect to three skew angles of -30°, 30° and 52.5° where the negative angle means the AG is skewed in the counter rotational direction. For all the cases, AG width of W/P is fixed at 30%. The Groove has a elliptical shape with major axis of 0.7C and minor axis of 0.53C. The downstream point of AG is located at 0.5C downstream of the tip LE and upstream point locates at 0.2C ahead LE. Case 5 with a negative skew angle re-injects flow in the rotational direction, generating a pre-swirl to the upstream, which is expected to reduce the flow incidence and mitigate stall. Case 6 and Case 7 having the skew angle in the rotation direction facilitates the extraction of tip vortical flow into groove and enhances the re-circulation.

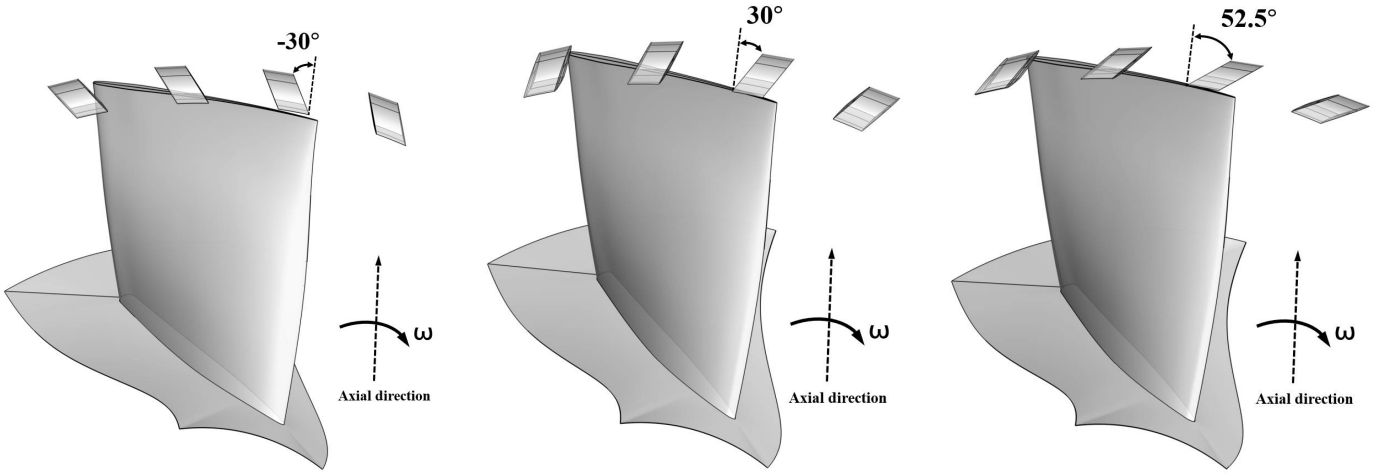

(a) Case 5 (b) Case 6 (c) Case 7

Figure 11: Configuration of the cases in skew angle study

Fig. 12 compares the compressor performance among the skewed AG cases and the baseline compressor. The highest stall margin improvement (SMI) of 7.4% is achieved by Case 7 with the skew angle of 52.5°. Case 5 with the negative skew angle AG only achieves a small improvement of 1.8% SMI. For the design point efficiency, all the three cases have a similar efficiency penalty of about 0.6%.

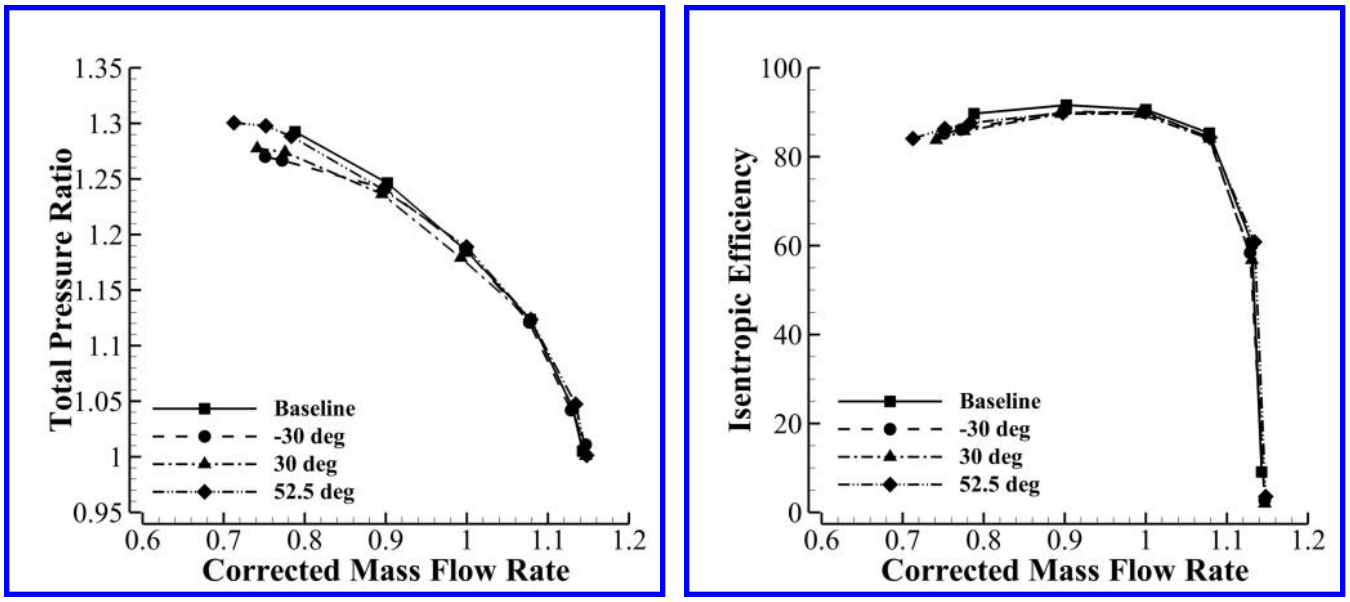

(a) Total pressure ratio (b) Isentropic efficiency

Figure 12: Computed speedlines of the axial groove with various skew angles

The alignment of rotating direction with the skew angle affects the flow extraction into the AG grooves. Fig. 13 shows the streamlines inside the AG of Case 5 and 7 which have the skew angle opposite to and in the rotating direction. As shown in Fig. 13 (b), the tip flow is extracted to the AG very smoothly in Case 7 due to the agreement between extraction angle and AG skew angle. The extraction angle (θ) is defined in Eq. 2, where U_{tip} is the circumferential velocity at tip and V_E is the velocity normal to groove slot. The Case 5 with the extraction angle opposite to the skew angle has the tip flow hitting on one side of AG wall and induces flow separation in the AG passage. The increased flow blockage inside the AG significantly reduces flow re-circulation, leading to an ineffective tip blockage mitigation. The reduced re-circulated flow is not able to generate enough pre-swirl to the upstream for swirl angle reduction. Fig. 14 shows that swirl angle of Case 5 is actually a little higher than that in Case 7 at tip region due to a larger tip blockage. Overall, Case 7 has the highest stall margin improvement with a low design point efficiency penalty and is therefore adopted as the optimum AG configuration for CFJ micro-compressor.

$$\theta = tan^{-1}(\frac{U_{tip}}{V_E}) \tag{2}$$

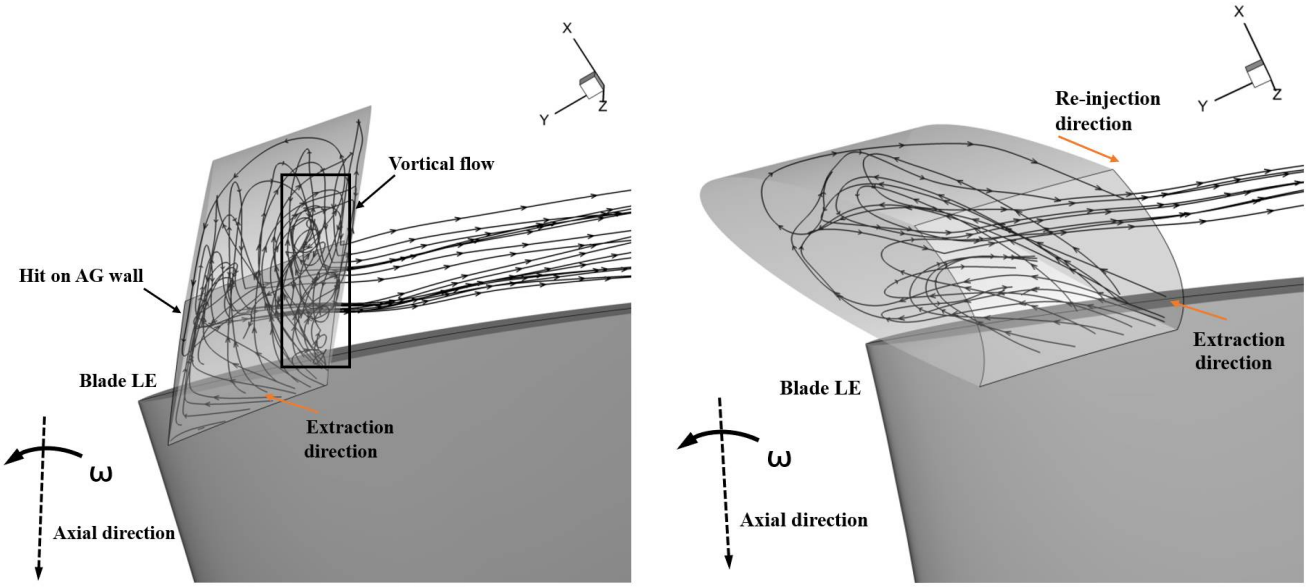

(a) Case 5 (b) Case 7

Figure 13: Streamlines inside AG

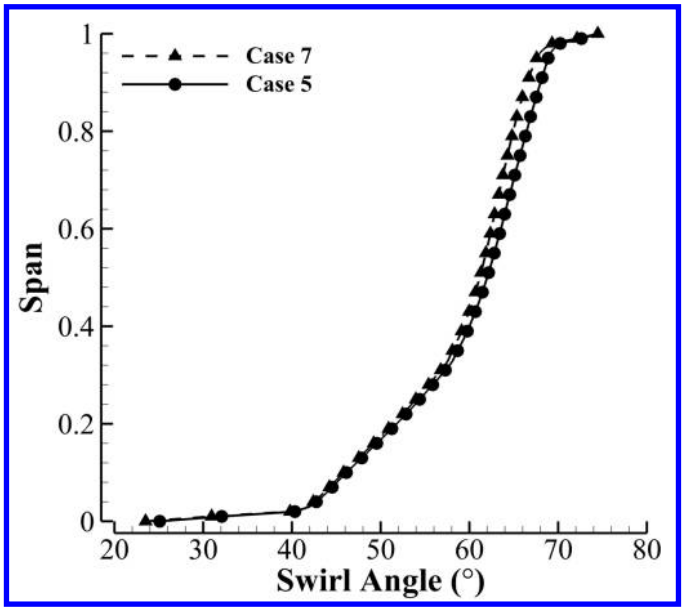

Figure 14: Swirl angle distribution upstream the rotor blade

6 Conclusion

This paper conducts numerical trade study of the axial groove (AG) casing treatment for micro-compressor actuators used for Co-Flow Jet (CFJ) active flow control. The optimal AG configuration is demonstrated to be very effective to be applied on CFJ micro-compressor that achieves SMI of 7.4% with a design point efficiency penalty of 0.6%. Three geometrical parameters are varied for the trade study, including: width, length and skew

angle. The numerical approach is validated with a tested micro-compressor using recirculating casing treatment. A very good agreement is achieved between the predicted speedlines and the measured results for the validated micro-compressor. For the width study, wide width with W/P of 60% possesses a higher stall margin improvement (SMI) of 10.1%, but an increased design point efficiency penalty of 4% also occurs. To preserve micro-compressor efficiency, the width W/P of 30% is adopted that has SMI of 3.1% with efficiency reduced by only 1.1%. Decreasing AG length to 0.7C (chord) results in a reduction of efficiency penalty while maintaining a similar SMI. However, a further decrease of AG length to 0.6C significantly hurts stall margin and reduces SMI by half. For the skew angle study, 52.5° is the optimal angle for AG to extract tip flow, which substantially enhances flow re-circulation and mitigates tip blockage. Overall, the optimum AG has the upstream point located at 0.2C ahead of LE and downstream point at 0.5C after the LE and has a W/P of 30%, a length of 0.7C with a skew angle of 52.5°.

References

[1] G.-C. Zha, B. F Carroll, C. D. Paxton, C. A. Conley, and A. Wells, "High-performance airfoil using coflow jet flow control," *AIAA journal*, vol. 45, no. 8, pp. 2087–2090, 2007.

[2] A. Lefebvre, B. Dano, W. Bartow, M. Fronzo, and G. Zha, "Performance and energy expenditure of coflow jet airfoil with variation of mach number," *Journal of Aircraft*, vol. 53, no. 6, pp. 1757–1767, 2016.

[3] G. Zha, W. Gao, and C.D. Paxton, "Jet Effects on Co-Flow Jet Airfoil Performance," *AIAA Journal*, vol. 45, pp. 1222–1231, 2007.

[4] G.-C. Zha, C. Paxton, A. Conley, A. Wells, nd B. Carroll, "Effect of Injection Slot Size on High Performance Co-Flow Jet Airfoil," *AIAA Journal of Aircraft*, vol. 43, pp. 987–995, 2006.

[5] Yang, Yunchao and Zha, Gecheng, "Super-Lift Coefficient of Active Flow Control Airfoil: What is the Limit?," *AIAA Paper 2017-1693, AIAA SCITECH2017, 55th AIAA Aerospace Science Meeting, Grapevine, Texas*, p. 1693, 9-13 January 2017.

[6] Z. Jinhuan, X. Kewei, Y. Yang, P. P. Ren Yan, and G. Zha, "Aircraft control surfaces using co-flow jet active flow control airfoil," *AIAA Aviation and Aeronautics Forum and Exposition 2018*, 2018.

[7] X. Kewei, Z. Jinhuan, and G. Zha, "Drag minimization of co-flow jet control surfaces at cruise conditions," *AIAA Science and Technology Forum 2019*, 2019.

[8] G. Zha, Y. Yang, Y. Ren, and B. McBreen, "Super-lift and thrusting airfoil of coflow jet actuated by micro-compressors," in *2018 Flow Control Conference*, p. 3061, 2018.

[9] C. Robison, "Design of a mixed flow fan," vol. PCA-211-3-rep1-1, PCA Engineering Limited, Feb. 23, 2017.

[10] C. Zwyssig, "Design of a mixed flow fan prototype," vol. PR-4241-011, Celereton, Oct. 24, 2017.

[11] K. Xu and G. Zha, "Design of high specific speed mixed flow micro-compressor for co-flow jet actuators," in *ASME Turbo Expo 2019: Turbomachinery Technical Conference and Exposition, Phoenix, Arizona, USA*, American Society of Mechanical Engineers Digital Collection,GT2019-90980, June 17-21, 2019.

[12] P. Patel and G. Zha, "Simulation of micro-compressor casing treatment using non-matching mesh interface," 2019. ASME No. GT2019-90977.

[13] X. Lu, W. Chu, J. Zhu, and Y. Zhang, "Numerical investigations of the coupled flow through a subsonic compressor rotor and axial skewed slot," *Journal of Turbomachinery*, vol. 131, no. 1, 2009.

[14] J. A. Streit, F. Heinichen, and H.-P. Kau, "Axial-slot casing treatments improve the efficiency of axial flow compressors: aerodynamic effects of a rotor redesign," in *ASME Turbo Expo 2013: Turbine Technical Conference and Exposition*, American Society of Mechanical Engineers Digital Collection, 2013.

[15] G. Legras, N. Gourdain, I. Tre´ binjac, and X. Ottavy, "Analysis of unsteadiness on casing treatment mechanisms in an axial compressor," in *Turbo Expo: Power for Land, Sea, and Air*, vol. 54679, pp. 163–175, 2011.

[16] H. Fujita and H. TAKATA, "A study on configurations of casing treatment for axial flow compressors," *Bulletin of JSME*, vol. 27, no. 230, pp. 1675–1681, 1984.

[17] I. Wilke and H.-P. Kau, "A numerical investigation of the flow mechanisms in a high pressure compressor front stage with axial slots," *J. Turbomach.*, vol. 126, no. 3, pp. 339–349, 2004.

[18] X. Lu, J. Zhu, C. Nie, and W. Huang, "The stability-limiting flow mechanisms in a subsonic axial-flow compressor and its passive control with casing treatment," in *ASME Turbo Expo 2008: Power for Land, Sea, and Air*, pp. 33–43, American Society of Mechanical Engineers Digital Collection, 2008.

[19] N. Djeghri, H. D. Vo, and H. Yu, "Parametric study for lossless casing treatment on a mixed-flow compressor rotor," in *ASME Turbo Expo 2015: Turbine Technical Conference and Exposition*, American Society of Mechanical Engineers Digital Collection, 2015.

[20] J. Du and J. R. Seume, "Design of casing treatment on a mixed-flow compressor," in *ASME Turbo Expo 2017: Turbomachinery Technical Conference and Exposition*, American Society of Mechanical Engineers Digital Collection, 2017.

[21] P. Harley, A. Starke, T. Bamba, and D. Filsinger, "Axial groove casing treatment in an automotive turbocharger centrifugal compressor," *Proceedings of the Institution of Mechanical Engineers, Part C: Journal of Mechanical Engineering Science*, vol. 232, no. 24, pp. 4472–4484, 2018.

[22] X. Kewei and G.-C. Zha, "Investigation of Recirculating Casing Treatment for Low-Pressure Ratio Mixed-Flow Micro-Compressor." ASME Paper GT2020-15822, ASME TURBO EXPO 2020, London, England, June 22-26, 2020.